RESEARCH PAPER

Electro-spinning of Cellulose Acetate/Au, Ag, Cu and Polyvinyl Acetate/Au, Ag, Cu Nanofibers for Wound Healing Applications

Davood Ghanbari *, Shiva Eghdamian, Amirhossein Amini

Department of Science, Arak University of Technology, Arak, Iran

ARTICLE INFO

ABSTRACT

One the most important property of a wound dressing is its antibacterial performance. Electrospun nanofibers showing great promise for fabricating nanostructured materials might help to wound dressing and skin engineering applications. The present study aimed to investigate and compare the wound healing potential of cellulose acetate (CA) nanofiber containing gold, silver, and copper also poly vinyl acetate (PVAc)/Au, PVAc/Ag and PVAc/Cu composite nanofibers. The samples with efficient antimicrobial capability was prepared via an electrospinning process. The comparison between these samples is aimed at selecting the best composite nanofibers for wound healing applications. For better comparison also aluminum and zinc nanoparticles were prepared by ball milling method, also amino-modified multiwall carbon nano tube were added to polymeric matrixes. Results approve gold, silver and copper have better antibacterial activities and we prepared their polymeric nano fibers composites. Various samples shows different morphology, structure, enhanced blood clotting ability and cell attachment as well as antimicrobial activity. Optimized combinations the samples were characterized by X-ray diffraction (XRD) pattern, field emission scanning electron microscopy (FE-SEM), transmission electron microscopy (TEM), and Fourier-transform infrared spectroscopy (FT-IR).

How to cite this article

INTRODUCTION

Among different nanomaterial, nanofibers are more potentially significant than other nanomaterials. Nanofibers are one dimensional material with less than 1µm (1000 nm) in diameter and the ratio of length to diameter is more than 100. Up to now nanofibers are made of materials such as artificial polymer, natural polymer, nanocomposite, semiconductor nanomaterial and etc. Large surface area to volume ratio, high interconnected porosity and mechanical resistance are the features that separate nanofibers from other nanomaterial [1-7], as many researches proved the high potential of nanofibers against the existing challenges in the medical field [8,9]. These prominent features of nanofibers have made them quite useful in drug delivery systems [10, 11], air (aerosol) filters [12] biosensors [13, 14], tissue engineering and tissue scaffolds [15, 16], covering and wound healing [17, 18], textile industry [19] and etc. Among the listed features the process of healing skin scars and wounds has highly appreciated since human skin is the widest organ which consists of three layers, dermis, epidermis and hypodermis. Therefore, process of wound healing is a complicated important biological

* Corresponding Author Email: *d-ghanbari@arakut.ac.ir*

process and an ideal healing process after a wound is caused, has four consecutive stages; hemostasis, inflammation, proliferation and maturation or remodeling. All the mentioned stages depending on the scar, could take up to months or years of treatment [20]. In addition to the proper medical treatments in this field, other effective treatments such as clearance and preventing infection against external microbial elements, is necessary since any open skin lesion due to environmental reasons such as warmth, moist and nutritious is a perfect place for microorganisms to grow and increase; through these open wounds bacteria can easily enter the body and reach lower levels of the tissue and create internal infections. Based on the cause of creation, wounds are categorized into various types such as type of injury, wound complication, wound's depth, time for wound healing and the color of infected tissue. Therefore, covering the wound is important based on its type [21]. Temporary dressing of a wound eases the process of healing but since it does not create stem cells for skin regeneration thus healing and covering wounds needs a more sophisticated procedure which can be designed by bioengineered knowledge. Materials for wounds healing are in different forms such as nanoparticles, nanofibers, hydrogels and etc. Ideal dressing for a wound has a similar tissue to that of human skin with a high absorption of exudates. Among all, nanofibers show the most promising results in wound healing and is a perfect dressing for wounds. Due to porous structure of nanofiber membranes, high surface area and structural similarities with extracellular matrix (ECM), they can be a perfect replacement for a better skin performance and treating superficial wounds or profound [22]. Although currently a lot of researches are out and many products have made based on nanofibers but they are still debatable in biomedical and healthcare fields and expanding researches for reaching a better target is essential. It is thought as with more progress in finding new ways for making nanofibers and expanding utilization, this technology will move towards commercialization more than ever. Because of their structure, nanofibers can keep moister and keep the scar moisturized during the healing process. Besides porous structure of nanofibers releases more oxygen in the wound's surface and protects the wound against dust particles [23].

Among different reported ways of creating nanofibers such as template synthesis, self-assembly, force spinning, phase separation and electrospinning, electrospinning draws more attention, since it can be used to create nanofibers for a wide range of materials such as polymer, metal oxide, carbon and composite with unique features like large surface area to volume ratio, inter\ intra fibrous porosity, superior tensile strength and many other features [24, 25]. This way leads to creating tissues with a diameter of less than micron to nanometer. Many of polymers, such as poly lactic acid (PLA) [26], poly (Ɛ-caprolactone), poly (lactide-co-glycoside) [27], polyvinyl alcohol (PVA) [28], polyvinyl acetate (PVAc) [29], cellulose acetate (CA) [30] and etc. have been successfully made by electrospinning method.

Electrospinning is an electro hydrodynamic (EHD) procedure which uses a high electric field (KV range) for rapid stretching of viscoelastic liquid and directing it to the collector. As seen in Fig. 1 high voltage power supply connected to the syringe's needle, is to make a polymer soluble jet; under high voltage a conical shaped drop is made from the polymer soluble in the syringe and through inducing ejection the liquid moves towards the counter electrode by the spinneret. As the voltage amplifies, the droplet slowly starts to stretch and meanwhile a jet is made from the drop that creates a good condition for making fibers so that with the increasing diameter of spiraling loops, jet turns longer and thinner, turns to solid and then placed on the collector connected to the ground. In other words, when applied high electric field (high voltage) overcomes the droplet's surface tension, a charged jet exits the polymer soluble inside the syringe and controlled by the applied electric field [31].

Electrospun nanofibers are quite practical in wound healing tissues since their size is compatible with human cells. Electrospun nanofibers' scaffolds are the cause of multiplication of skin cells such as fibroblasts, keratinocytes and facilitate the secretion of critical ECM components like collagens and help heal injured tissues. Electrospun nanofiber mats is an ECM like matrix with high interconnected porosity, perfect absorption, hydrophilic and high water absorbance capacity between 18 and 231% more than thin films are made from the same polymers.[32]

Among the biocompatible polymers for creating electrospun nanofibers, CA as biopolymer nanofibers is noted for many applications including

medical purposes, hydrophilicity, transporting liquid, great compatibility with human body's condition, solubility in organic solvents, non-toxic, economical in effective for wounds healing. Still with so many applications due to low tensile strength and weak resistance, CA is not appropriate to be used in clinics and limits its functions in human skin regeneration. Due to this CA is combined with other polymers such as poly (Ɛ- caprolactone), polyurethane, gelatin or combined with metal nanoparticles doped inside (within) electrospun CA nanofibers to decrease the limitations when it is used singly and creates a better function in tissue regeneration [33-38]. Composite polymer nanofibers show anti-bacterial qualities against gram-positive and gram-negative bacteria.

Also, polyvinyl acetate (PVAc) is often used as a carrier polymer for the creation of inorganic nanofibers. PVAc is one of the most important artificial polymers with lots of use in medical area; PVAc is highly noted due to their good biocompatibility with blood, tissue and body fluids. PVAc includes acetate functional groups which is common in biological metabolites systems [39, 40].

Furthermore, nanoparticles play an important role in medical areas, wound healing and skin reparation due to their function as an antioxidant.

Among metal nanoparticles, silver nanoparticles play an important role in healing wounds due to their lower toxicity, safety, cost-effectiveness and broad spectrum resistance against different microorganisms. Ag nanoparticles (Ag NPs) have a high surface to volume ratio which increases the effectiveness and wound healing process. Moreover, based on the researches in this field, silver nanoparticles have the ability to block respiratory tracts of living cells and reproliferation skin cells (fibroblasts and keratinocytes) will lead to reparation and healing of the skin. They also show strong antibacterial effects against gram-negative/positive bacteria [41, 42]. Gold nanoparticles are also known as the most compatible and stable nanoparticles due to their unique qualities. Au nanoparticles (Au NPs) have noted for their optical, chemical, magnetic features and etc. for biological functions. Au NPs also have antimicrobial, antioxidative effects and high surface reactivity in healing wounds and reparation of injured tissues. Au NPs also have an important role in exuding proteins which because of their antiangiogenic and anti-inflammatory activities are one of the most important options in reparation of injured skin tissue [43, 44]. Copper is among the elements with antioxidants, matrix metalloproteases stability and direct role in angiogenesis in human skin; for this reason, lack of this element postpones the
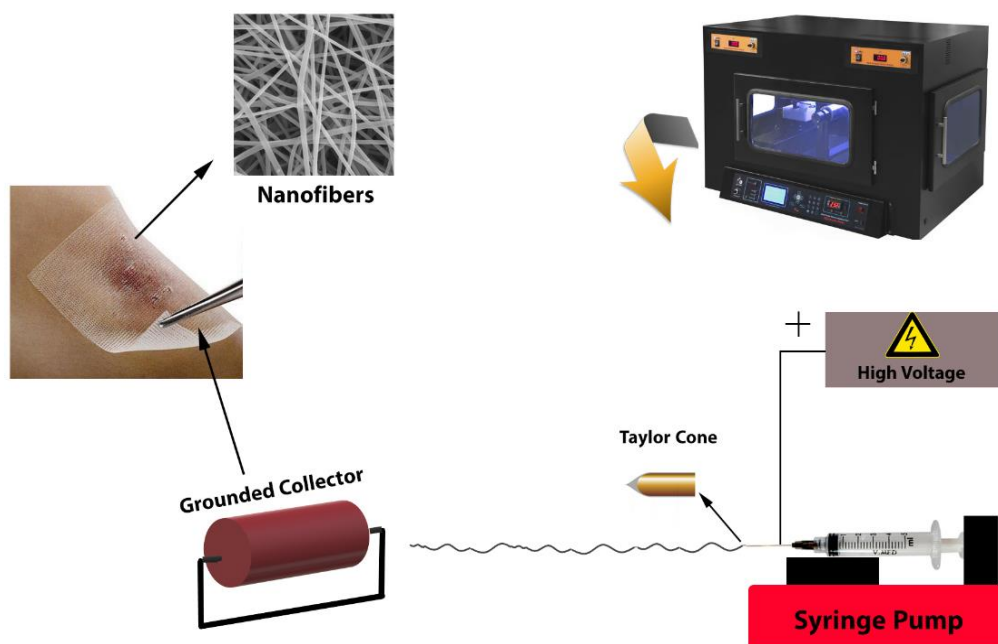

Fig 1. Schematic of electrospinning setup

scar-healing process. Based on researches in this field it was also observed that Cu nanoparticles (Cu NPs) accelerate and sustain the scar-healing in the first the stages of healing process due to antibacterial activities. Cu NPs are also noted for their high redox features and low cost [45, 46]. Also, since discovering Carbon Nanotubes (CNTs) in 1991 by Lijima [47] they are largely used in medical functions. CNTs can attach to proteins and receptors on the cell membrane. Because of their tube like shape, they offer a high surface area. With due attention to researches in wound healing field, composite polymer nanofibers have effective (the best) influence on wounds healing process and controlling microbe's growth inside and around the wounds. In the current research, considering hopeful potentials of composite nanofibers in wound healing, for analyzing the optimal sample for wound dressing material, with the goal of increasing hydrophilicity, antibacterial activity, multiplication of human skin cells and the ability of blood clotting, first a comparison between Au, Ag, Cu, Zn and Al NPs was done and then CA/Ag, CA/Au, CA/Cu, PVAc/Cu, PVAc/Ag and PVAc/Au composite nanofibers were compared. Also sample's antibacterial effects, structure, compatibility, morphology were investigated using electrospinning technique. For increasing

conductivity modified carbon CNTs were used. In this study from Fourier transform infrared (FT-IR), emission scanning electron microscopy (FE-SEM), x-ray fluorescence (XRF), x-ray diffraction (XRD), UV/Vis spectroscopy and Transmission Electron Microscopy (TEM) are used for precise analysis of tested samples.

MATERIALS AND METHODS
Preparation of Au, Ag, Cu, Zn, Al nanoparticles.

As shown in Fig. 2.a, for making gold nanoparticles, first 0.01 mol of was placed in the beaker and for dissolving , 200cc of deionized water was added. Then a magnet was placed in the beaker and the beaker was placed on a heater stirrer. At the end, tri-sodium citrate ($Na_3C_6H_5O_7$) in 50° C temperature was added to the soluble so that its color turns into red wine; in this stage, since size of the droplet is important, it is necessary for soluble's color to remain the same. For making silver nanoparticles, first 0.01 mol of was poured in the beaker then 200cc of deionized water was added to for dissolving and was placed inside the beaker. Then a magnet was placed inside and the beaker was placed on the heater stirrer with the previous specifications. After it was cleared, the soluble was exposed to ultrasound waves and 150W power. Inside another
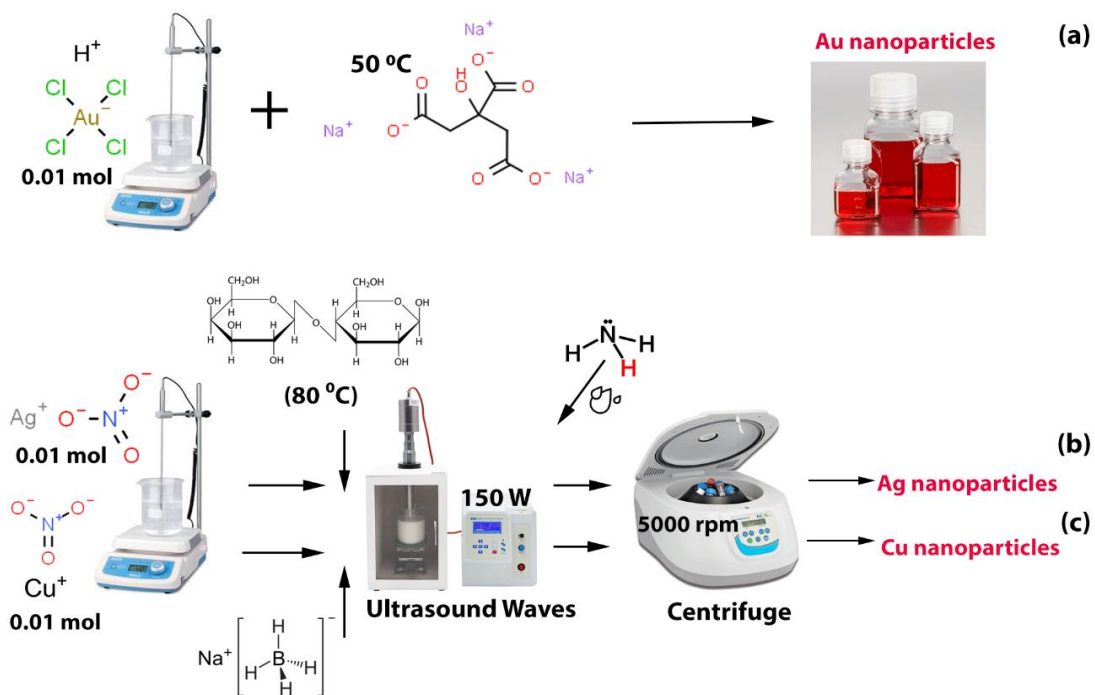

Fig. 2. Schematic route for preparation of a) Au NPs b) Ag NPs and c) Cu NPs

container, precipitating agent of soluble that are lactose and ammonia () were dissolved in 50cc of water; main reason for using receiver sediment is nucleation, creating nanomaterial and the transforming to suspension; while the ultrasound waves apparatus was running, for precipitating, lactose and ammonia were slowly added to the in 80° C, reason for this temperature is for better precipitating of silver. Then the collected sediment was placed inside a centrifuge with 5000 rmp and washed with water and acetone so that only silver

sediment nanoparticles remain. The procedure for making silver nanoparticles is shown in Fig. 2.b. For making copper nanoparticles, was placed inside the beaker and then 200cc of deionized water was added inside the container. Then a magnet was placed and the beaker was placed on the heater stirrer with the same specifications. After making transparence in soluble, it was exposed to ultrasound waves with previous power settings. First NaBH$_4$ as precipitating agent was dissolved in under the nitrogen atmosphere and added to
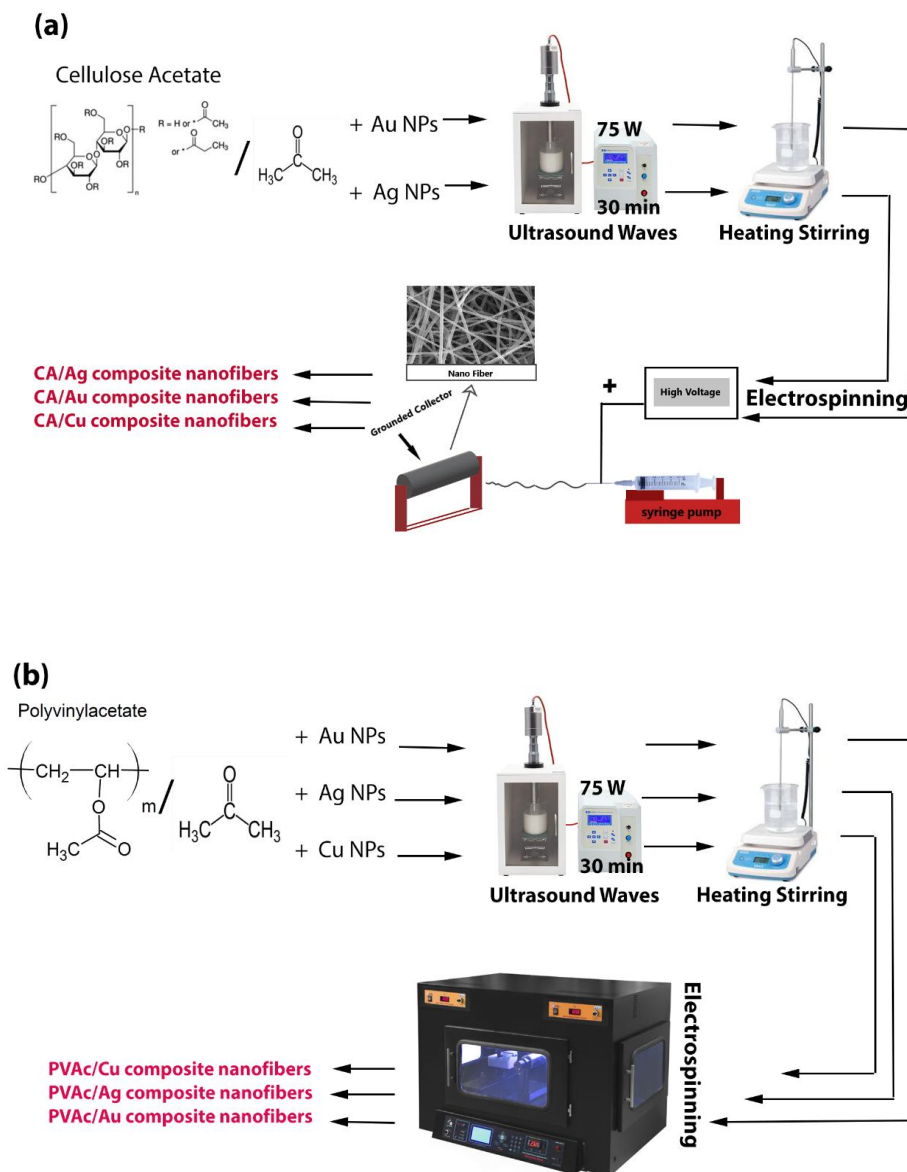

Fig. 3. Schematic route for preparation of CA/Au, CA/Ag composite nanofibers and b) PVAc/ Au, PVAc/ Ag, and PVAc/ Cu composite nanofibers

until the sediment's color turned copper. Then the sediment was placed inside the centrifuge with 5000 rmp and washed with deionized water for removing the extra materials and eventually copper nanoparticles were made. Procedure of making Cu NPs is shown in Fig. 2.c. Also for comparison Zn and Al nanoparticles were made by a balling mill with specifications of inert atmosphere and zirconium balls (2000 rpm) .Moreover, for better comparison also modified-CNTs were added to polymer matrix and antibacterial test was examined.

CA/Au, CA/Ag, CA/Cu and PVAc/Au, PVAc/Ag, and PVAc/Cu composite nanofibers fabrication

As shown in Fig. 3.a, for synthesizing CA, 5g of CA was dissolved inside 15cc of acetone to turn into jelly form. Then 5% of Au NPs made from previous stage was added to polymer. Combination of CA with Au NPs was placed inside ultrasound waves with 75W power for 30 minutes. Ultrasonic waves have been used to better disperse nanoparticles in nanofibers. Beside dispersion application, ultrasonic waves also can decrease size of the particle by micro-jets. Then was placed in the heater stirrer for 5 hours. After 5 hours, for de-bubbling, the sample was inside the heater stirrer for one hour in a stable state and without any changes; meanwhile, to prevent the soluble from evaporating, paraffin was placed on top. Then the syringe filled with the soluble was placed inside the electrospinning device (ES1000 model, company of FNM) with 13 KV voltage. Distance between the nozzle and collector was 20 cm for the sample and temperature was set to about 30 ° C; it was spinned with 0.01 ml/min ratio. Then composite nanofibers CA/Au was picked up from the plate with a cutter. The same method was used for making composite nanofibers containing silver and copper nanoparticles.

As shown in Fig. 3.b, for synthesizing PVAc polymer, 5gr of that was dissolved in acetone to turn into jelly form. Then 5% of AuNPs made from previous stage was added to the polymer. The sample was placed inside ultrasound wave instrument with 75W for 30 minutes. Then, the sample was placed inside heater stirrer for 5 hours. After 5 hours, for de-bubbling, sample was placed inside heater stirrer in a stable state, meanwhile, to prevent the soluble from evaporating, paraffin was placed on it. Then a syringe filled with the soluble was placed inside the electrospinning machine with previous specifications and after spinning,

PVAc/Au composite nanoparticles was taken from the plate with a cutter. With the same procedure PVAc/Ag and PVAc/Cu composite nanofibers were made.

Characterization

Prepared nanoparticles and nanocomposite fibers morphology, using field emission scanning electron microscopy (FESEM: MIRA3 model, made by company TESCAN) was done and the diameter of nanoparticles and nanofibers was observed. Images of TEM using transmission electron microscope (EM 208S model, point to point (resolution, 0.45 nm), Tungsten Filaments (electron gun), voltage: 100KV) were checked for Au and Ag NPs samples. X-ray diffraction analysis (XRD) using X, pert PW3040/60 Philips Holland with chromium radiation (= 2.289 Å) was done to analyze nanoparticles' crystal structure. Fourier transform infrared spectroscopy (FTIR) for studying evaluate the chemical structural properties was done by ALPHA model from Bruker Company. Spectra were obtained over a range of 400–400 at room temperature. For analyzing and detecting elements, X-Ray Fluorescence (XRF) apparatus (BRA-135F model made by Bourevestnik Company) was used. UV visible spectroscopy is one of the most prevalently used analytical techniques for structural characterization of Ag, Au and Cu NPs. UV–VIS absorption spectra were recorded on a UV–Vis spectrophotometer (SCO TECH, SPUV -21 model).

RESULTS AND DISCUSSION

XRD pattern of Au NPs is shown in Fig. 4.a The pattern of as-prepared Au NPs is indexed as a pure cubic phase (space group: Fm3m, space group number: 225) which is very close to the literature values (ICDD, PDF-2 NO. 00-004-0784) the narrow sharp peaks indicate that Au NPs are well crystallized. The diffraction peak of gold nanoparticles observed at the 2θ values of 58°, 68°, and 105° which are corresponding to the set of lattice planes (111), (200) and (220), respectively. In the present study, the observation of strong peaks indicates the synthesized Au NPs are pure and crystalline in nature.

XRD pattern of Ag NPs is illustrated in Fig. 4.b Peaks of Ag NPs are observed. This analysis was performed to identify the crystalline nature and structure of the silver nanoparticles. The diffraction peak of synthesis of Ag nanoparticles

observed at the 2θ values of 58.01°, 68°, and 104° which are corresponding to the set of lattice planes (111), (002) and (022). The results show that there were no other peaks observed in the XRD spectrum indicates the synthesized Ag NPs is pure. Pure cubic phase of silver (ICDD, PDF-2 NO. 96-150-9867, space group is Fm -3m and number is 225) can be observed in this pattern. Therefore, XRD confirms that Ag NPs had cubic structure with peaks sharpness due to nano-sized structure of the nanoparticles.

XRD pattern of Cu NPs is shown in Fig. 4.c, to obtain evidence that the Cu NPs formed, X-ray diffraction was performed after sample preparation. The pattern of as-prepared Cu NPs is indexed as a pure cubic phase (space group: Fm-

3m) which is very close to the reference code (ICDD, PDF-2 NO. 01-085-1326). Bragg's reflections for Cu NPs are observed in XRD pattern at representing (111) and (200) planes and revealed that the resultant particles were pure metallic Cu. The sharp peaks in the pattern indicated the existence of Cu NPs and its crystalline nature.

For better comparison also aluminum and zinc nanoparticles were prepared by ball milling method, also amino-modified multi wall carbon nano tube were added to polymeric matrixes. Results approve Au, Ag and copper have better antibacterial activities and we prepared their polymeric nano fibers composites. XRD pattern of synthesized Zn NPs was obtained by ball milling as displayed in Fig. 5. a the crystalline peaks
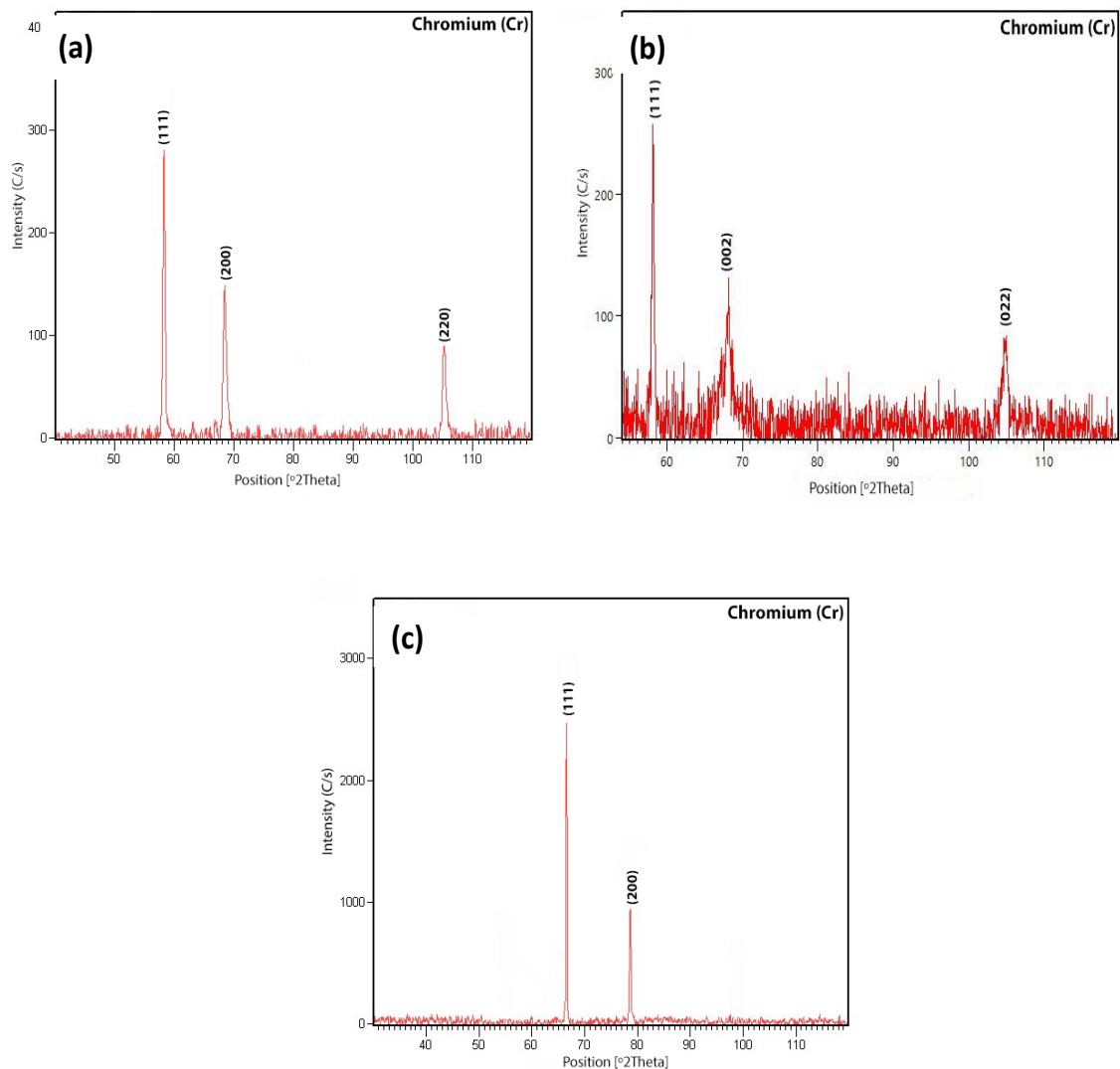

Fig. 4. XRD pattern of (a) Au, (b) Ag and (c) Cu nanoparticles.

positioned at (2θ) peaks angles of 55°, 59°, 66°, 85°, 117°, and 118° correspond to the reflection from (002), (100), (101), (102), (103) and (110) crystal planes, respectively. Pure hexagonal phase of Zn (ICDD, PDF-2 NO. 01-087-0713, space group is P63/mmc, number is 194) can be observed in this pattern. The absence of any other peak in the XRD patterns of Zn NPs illustrates purity of nanoparticles.

Fig. 5.b shows the x-ray diffraction pattern of Al NPs, the absence of any other impurities peaks confirms the high purity of the Al NPs structure. Also, the sharp and intense peaks demonstrated good crystallinity. It is observed that sample is in well agreement with the reference cubic Al structure (ICDD, PDF-2 NO. 01-085-1327, space group: Fm-3m, space group number: 225).

Studies have clearly shown that NPs are an important platform for skin wounds treatment , FE-SEM images of Au NPs are shown in Fig. 6.a, b that confirm preparation of gold nanoparticles. Gold nanoparticles are so fine, they are not clearly visible in SEM images.

The surface morphology of Ag NPs was investigated using FE-SEM (Fig. 6.c, d). As the results confirm mono-disperse nanoparticle with average size less than 30 nm were synthesized.

The morphology of Cu NPs was investigated by FE-SEM. Fig. 6.e, f shows copper nanoparticles. In general, in recent researches have been revealed that Cu NPs increased endothelial, keratinocyte, and fibroblast cell migration [46].

FE-SEM images of Zn NPs that were prepared by ball milling method are shown in Fig. 7.a, b

Images approve suitable and fine mono-disperse nanoparticles with mediocre size less than 90 nm were prepared.

Fig. 7.C, d depict various magnification FE-SEM images of Al NPs obtained from ball milling that confirm preparation of nanostructures, average diameter size is about 100 nm.

Fig. 8 shows FE-SEM of carbon nanotubes that have used to improved conductivity properties, modified CNTs without agglomeration were regularly formed.

The nano-composite mats were investigated using FE-SEM for evaluating the morphological details. According to Fig. 9.a, b electrospun PVAc/Au nanocomposite fibers are randomly oriented including continuous fibers with smooth surface and diameters ranging from 100 nm to 200 nm, because gold nanoparticles are so fine, they are not visible on PVAc nanofibers. PVAc/Au nanofibers had a smooth surface, uniform fiber diameter, and favorable morphology. Since the viscosity, weight of the molecule, surface charge, dielectric constant and tension affect the nanofiber size, so for the preparation of all composite nanofibers in this study, a voltage of 13 kV and a distance of 20 cm were used.

Fig. 9.c, d depict FE-SEM (various places of sample and different magnifications) of PVAc nanofibers/Ag that also were synthesized at 13KV, 20 cm, as the SEM confirms size of the nanostructures are less than 150 nm. Images obviously show nanoparticles on the surface of the polymers. Ag NPs distributed inside the produced PVAc nanofibers as very little spherical spots.
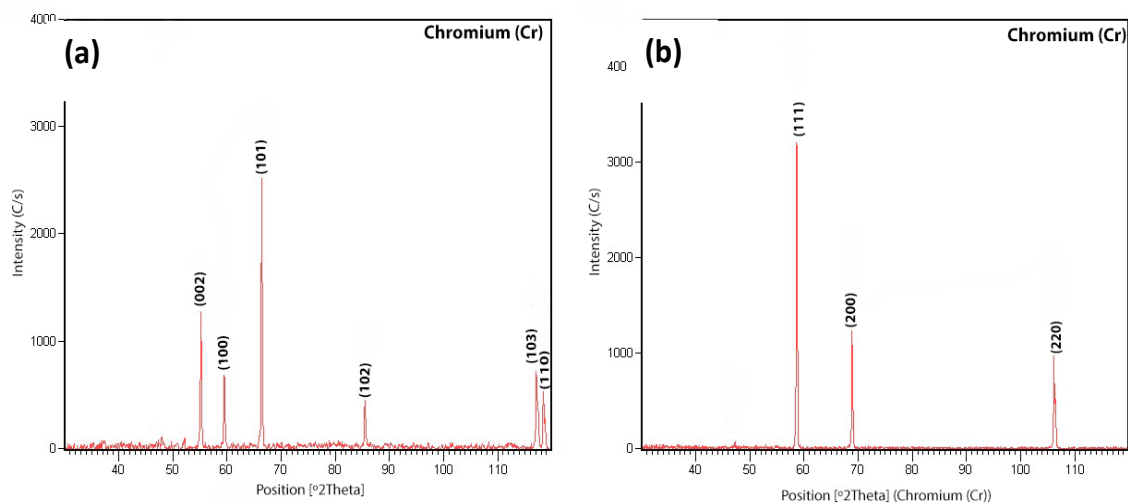

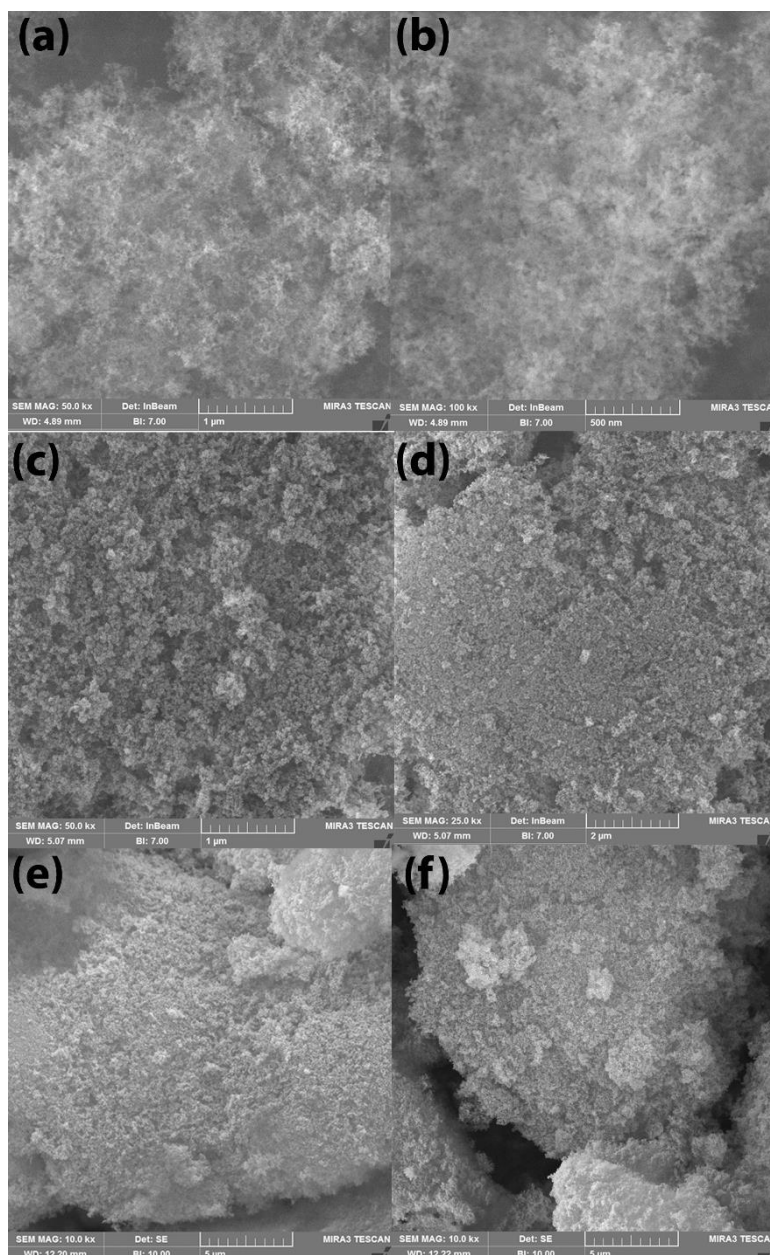Fig. 5. XRD pattern of (a) Zn and (b) Al nanoparticles.

Fig. 6. FE-SEM images of (a), (b) Au, (c), (d) Ag and (e), (f) Cu nanoparticles.

Diameters of the PVAc/Au composite nanofibers were higher in comparison to PVAc/Ag sample.

FE-SEM images of PVAc/Cu nanofibers that have achieved at 13 kV and 20 cm distance is illustrated in Fig. 9.e, f Product obtained shows at these images which contain some Cu beads and a lot of PVAc nanofibers.

The CA was chosen as a polymer for incorporation of Au NPs and Ag NPs to prepare a nanofiber composite for antibacterial applications.

The results given in Fig. 10.a, b show regular CA/Au composite nanofibers. It is clear from these figures that no phase separation has been observed and the homogeneity of the obtained Nanofiber can be easily observed and the doping of Au has been proved. The fibers were randomly oriented with almost uniform diameters along their lengths.

By FE-SEM analysis, the morphological characteristics of developed CA/Ag were studied in Fig. 10.c, d, silver nanoparticles have significantly
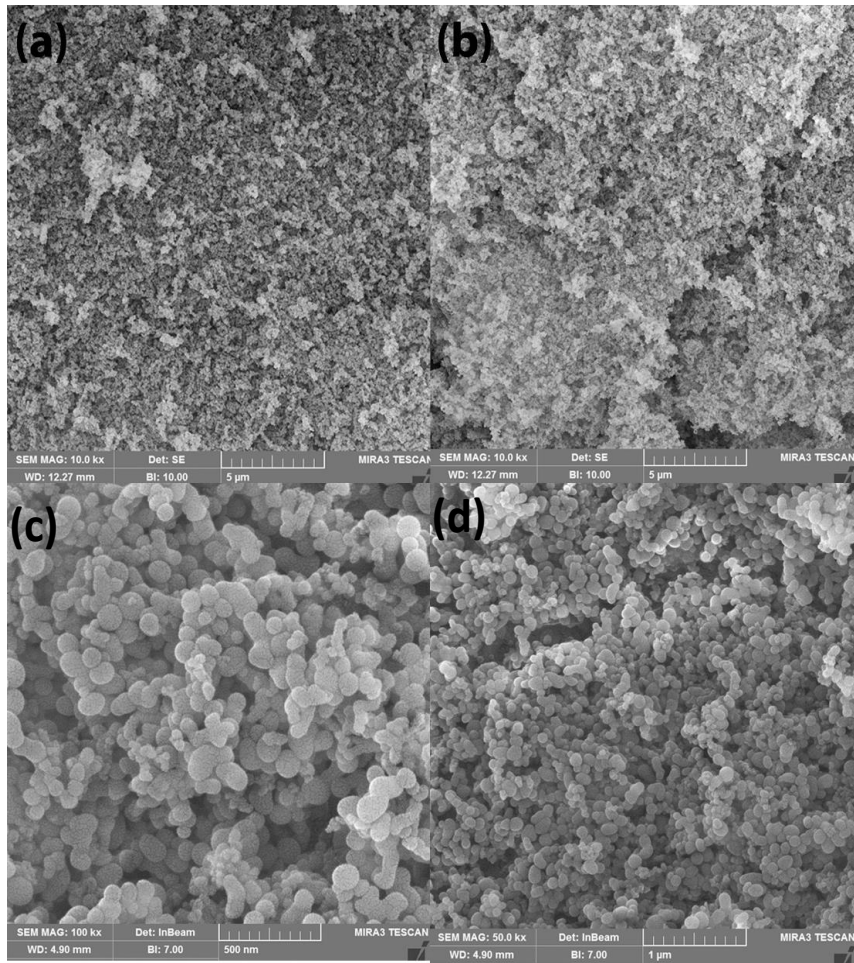
Fig. 7. FE-SEM images of (a), (b) Zn and (c), (d) Al nanoparticles.
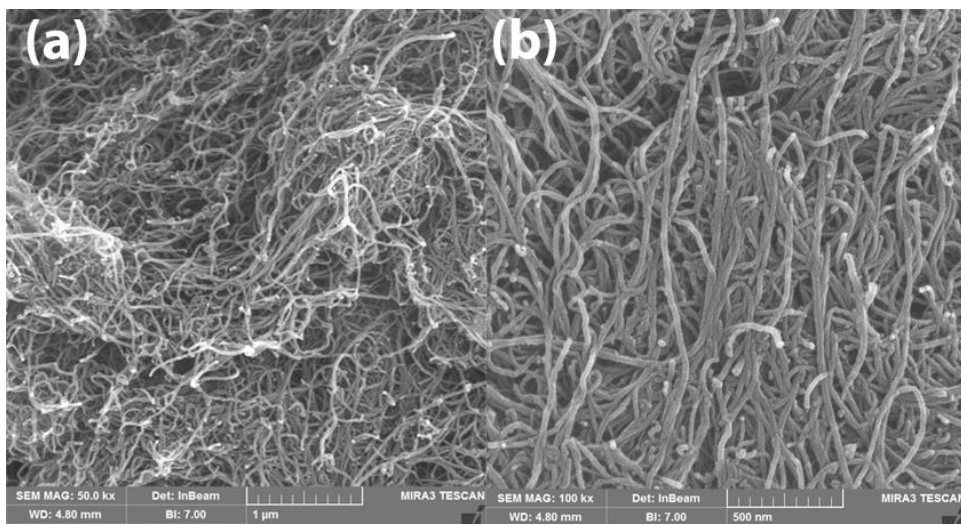

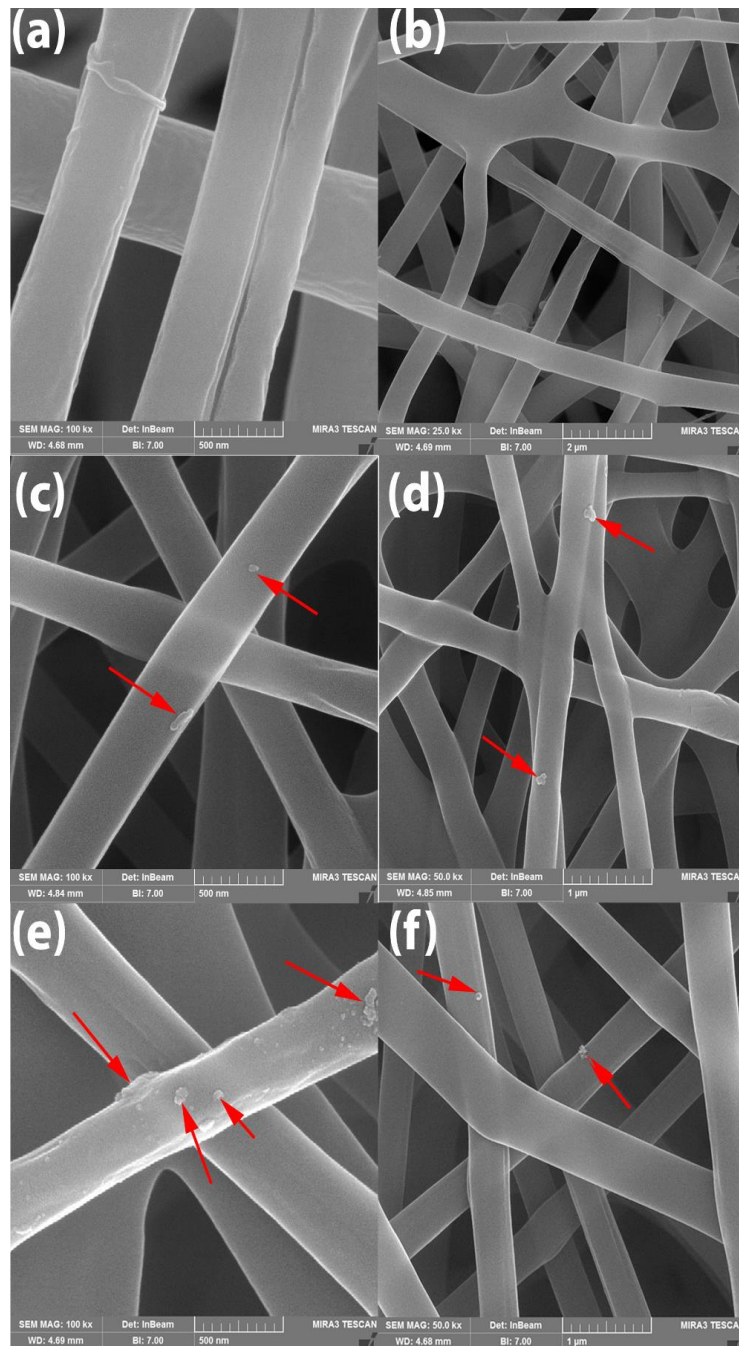Fig. 8. FE-SEM images of carbon nanotubes.

Fig. 9. FE-SEM images of (a), (b) PVAc/ Au, (c), (d) PVAc/ Ag and (e), (f) PVAc/ Cu composite nanofibers.

accumulated in CA nanofibers.

SEM images of composite nanofibers confirm that by increasing charge density of nanoparticles in the electrospinning, the nanofibers diameters decrease. It is because they ejected with stronger elongation force in electric field and thinner nanofibers are prepared. According to previous published works, viscosity of solution has a major role in size of fiber and morphology in polymer fiber spinning process [48].

Synthesis of Au NPs and Ag NPs was further studied by TEM observations. Transmission
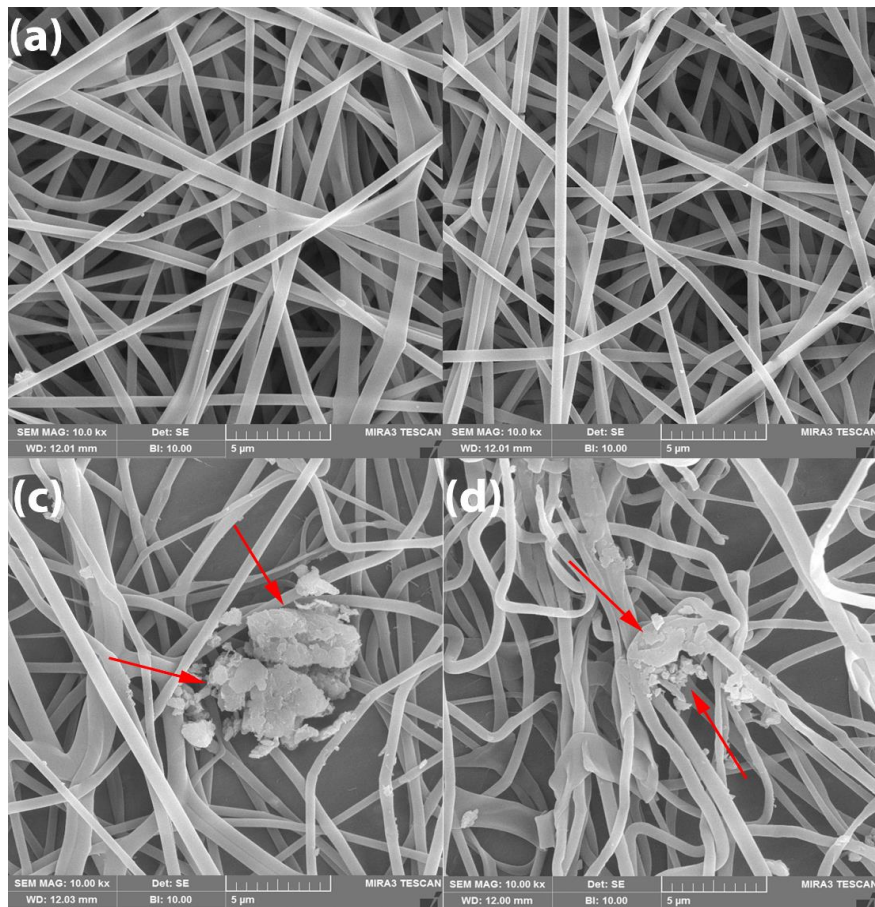
508

Fig. 10. FE-SEM images of (a), (b) CA/Au and (c), (d) CA/Ag composite nanofibers.

electron microscopy was used for precise investigation of Au NPs and Ag NPs. Fig. 11(a) and (b) illustrate TEM images of gold and silver nanoparticles, respectively. Due to the smaller size of gold nanoparticles than silver nanoparticles, 300 nm magnification was chosen for gold TEM
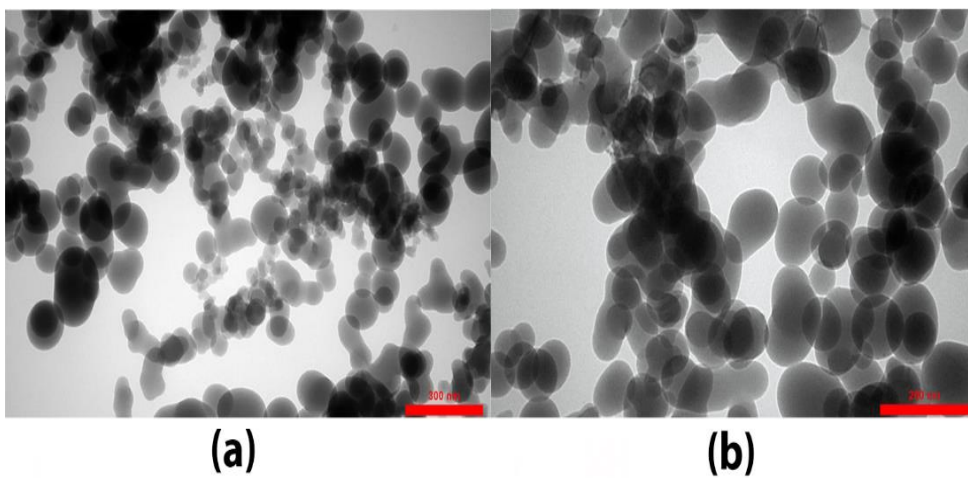

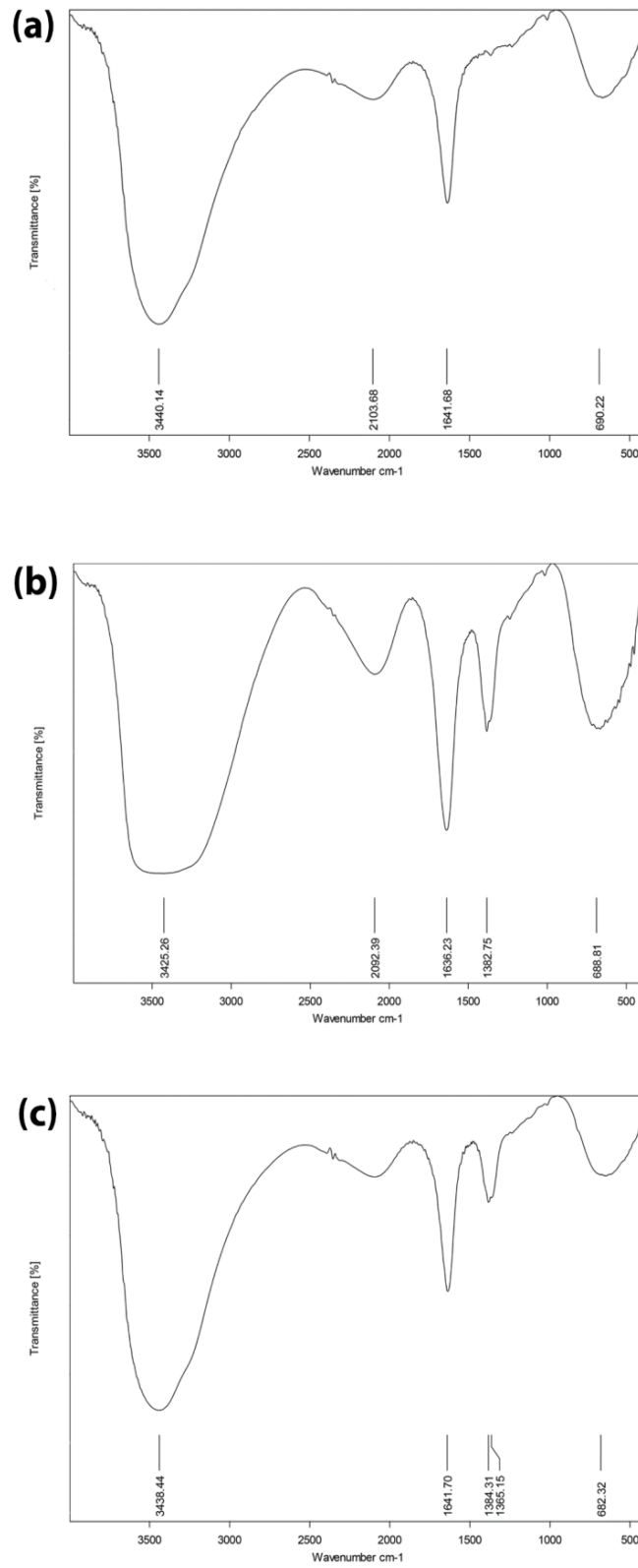Fig. 11. TEM images of (a) Au and (b) Ag nanoparticles.

Fig. 12. Fourrier transform infra-red of (a) Au, (b) Ag and (c) Cu nanoparticles.
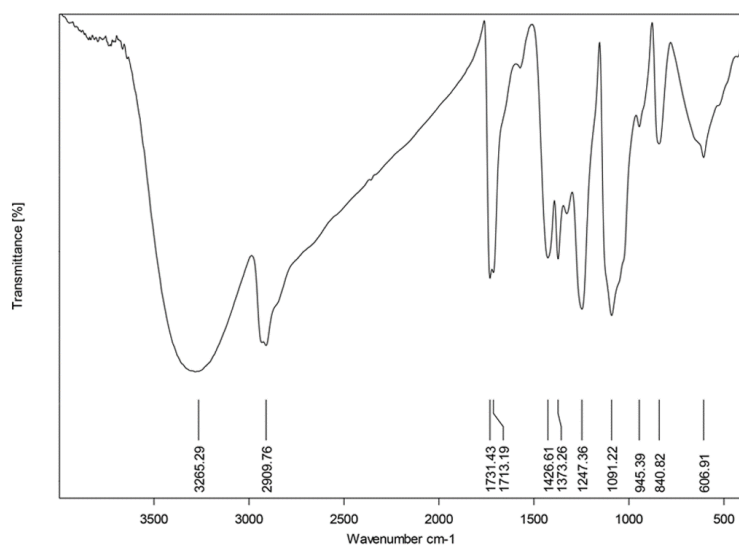
Fig. 13. . Fourrier transform infra-red of the CA/Au nanofiber.

imaging and 200 nm magnification for silver TEM imaging. The Au NPs had sizes between 50nm ~100nm and for Ag NPs average size is less than 100 nm. These spherical Au and Ag NPs with these particle size ranges are suitable for wound healing applications and can be made of electrospun nanofibers. Furthermore, in these images, some of Au and Ag NPs were in non- spherical shaped due to two or three spherical particles interference through nucleation process.

Fourrier transform infra-red of the Au, Ag and Cu nanoparticles are shown in Fig. 12 a-c respectively, peaks at 670 cm^{-1} is for metal-oxygen bonds and wide absorption at 3416 cm^{-1} is related to O-H bond. Absorption peaks around 1600cm^{-1} are related to carbonyl groups of tri sodium citrate as a precipitating and capping agent. Fig. 13 depicts Fourrier transform infra-red of the CA/Au nanofiber.As can be seen, the absorption bands of samples are in the identical range. The peak appears at about 600 cm^{-1} corresponds to tensile vibration mode of the metal- oxygen bond. The

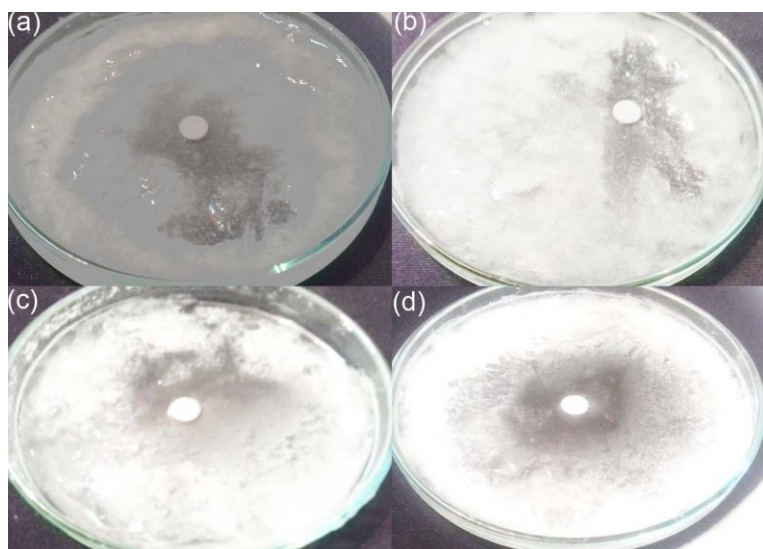
Fig. 14. Inhibition zone for (a) gold nanoparticles (b) silver nanoparticles (c) copper nanoparticles (d) CA/Ag nanocomposite.

peaks of 945 and 1091 cm^{-1} represents the C-O bonds. Absorption at 1713 and 1731 cm^{-1} related to C=O stretching bonds, bending vibration of C-H and C=O are about 1247, 1373 and 1426 cm^{-1}, which are related to polymer matric. As shown in the figure the absorption band at 3265cm^{-1} and 2909 are for tensile vibration of the O-H and C-H bonds respectively.

In antibacterial test, the disk diffusion is used to determine the susceptibility of clinical isolates of bacteria to different antibiotics. Applying an effective antibacterial nanoparticles leads to a large zone of inhibition, while an ineffective nanoparticles may not affect bacterial growth at all. Inhibition zone for gold nanoparticles, silver nanoparticles, copper nanoparticles and CA/Ag nanocomposite are shown in Fig 14a-d respectively.

CONCLUSION

Cellulose acetate nanofiber containing gold, silver and copper nanoparticles, also poly vinyl acetate (PVAc)/Au, PVAc/Ag and PVAc/Cu composite nanofibers was studied and were compared to each other's for wound healing potential. The samples with efficient antimicrobial capability was prepared via an electrospinning process. Various samples shows different morphology, structure, enhanced blood clotting ability and cell attachment as well as antimicrobial activity. X-ray diffraction pattern confirm crystallinity, field emission scanning electron microscopy and transmission electron microscopy approve particle and fiber size, Fourier-transform infrared spectroscopy show bonds and purity of the samples without major impurities. For better comparison also aluminum and zinc nanoparticles were prepared by ball milling method, also amino-modified multiwall carbon nanotube were added to polymeric matrixes. Results approve Au, Ag and copper have better antibacterial activities and we prepared their polymeric nanofibers composites.

CONFLICT OF INTEREST

The authors declare that there is no conflict of interests regarding the publication of this manuscript.

REFERENCES

1. Shams HR, Ghanbari D, Salavati-Niasari M, Jamshidi P. Solvothermal synthesis of carbon nanostructure and its influence on thermal stability of poly styrene. Composites Part B: Engineering. 2013;55:362-367.

2. Mirdamadian Z, Ghanbari D. Synergistic Effect Between Sb$_2$O$_3$ Nanoparticles–Trichloromelamine and Carbon Nanotube on the Flame Retardancy and Thermal Stability of the Cellulose Acetate. Journal of Cluster Science. 2013;25(4):925-936.

3. Ebadi M, Mirdamadian Z, Ghanbari D, Moradi L. The Effect of Aminated Carbon Nanotube and Phosphorus Pentoxide on the Thermal Stability and Flame Retardant Properties of the Acrylonitrile–Butadiene–Styrene. Journal of Cluster Science. 2013;25(2):541-548.

4. Kenry, Lim CT. Nanofiber technology: current status and emerging developments. Prog Polym Sci. 2017;70:1-17.

5. Ahmadian-Fard-Fini S, Ghanbari D, Amiri O, Salavati-Niasari M. Electro-spinning of cellulose acetate nanofibers/Fe/carbon dot as photoluminescence sensor for mercury (II) and lead (II) ions. Carbohydr Polym. 2020;229:115428.

6. Barhoum A, Rasouli R, Yousefzadeh M, Rahier H, Bechelany M. Nanofiber Technology: History and Developments. Handbook of Nanofibers: Springer International Publishing; 2018. p. 1-42.

7. Alghoraibi I, Alomari S. Different Methods for Nanofiber Design and Fabrication. Handbook of Nanofibers: Springer International Publishing; 2018. p. 1-46.

8. Hassiba AJ, El Zowalaty ME, Nasrallah GK, Webster TJ, Luyt AS, Abdullah AM, et al. Review of recent research on biomedical applications of electrospun polymer nanofibers for improved wound healing. Nanomedicine. 2016;11(6):715-737.

9. Rasouli R, Barhoum A, Bechelany M, Dufresne A. Nanofibers for Biomedical and Healthcare Applications. Macromol Biosci. 2018;19(2):1800256.

10. Kajdič S, Planinšek O, Gašperlin M, Kocbek P. Electrospun nanofibers for customized drug-delivery systems. J Drug Deliv Sci Technol. 2019;51:672-681.

11. Malik R, Garg T, Goyal AK, Rath G. Polymeric nanofibers: targeted gastro-retentive drug delivery systems. Journal of Drug Targeting. 2014;23(2):109-124.

12. Liu C, Hsu P-C, Lee H-W, Ye M, Zheng G, Liu N, et al. Transparent air filter for high-efficiency PM2.5 capture. Nature Communications. 2015;6(1).

13. Ahmadian-Fard-Fini S, Ghanbari D, Salavati-Niasari M. Photoluminescence carbon dot as a sensor for detecting of Pseudomonas aeruginosa bacteria: Hydrothermal synthesis of magnetic hollow NiFe$_2$O$_4$-carbon dots nanocomposite material. Composites Part B: Engineering. 2019;161:564-577.

14. Sapountzi E, Braiek M, Chateaux J-F, Jaffrezic-Renault N, Lagarde F. Recent Advances in Electrospun Nanofiber Interfaces for Biosensing Devices. Sensors (Basel, Switzerland). 2017;17(8):1887.

15. Li T, Tian L, Liao S, Ding X, Irvine SA, Ramakrishna S. Fabrication, mechanical property and in vitro evaluation of poly (L-lactic acid-co-ε-caprolactone) core-shell nanofiber scaffold for tissue engineering. J Mech Behav Biomed Mater. 2019;98:48-57.

16. Nemati S, Kim S-J, Shin YM, Shin H. Current progress in application of polymeric nanofibers to tissue engineering. Nano convergence. 2019;6(1):36-36.

17. Zhang S, Ye J, Sun Y, Kang J, Liu J, Wang Y, et al. Electrospun fibrous mat based on silver (I) metal-organic frameworks-polylactic acid for bacterial killing and antibiotic-free wound dressing. Chem Eng J. 2020;390:124523.

18. Zehra M, Zubairi W, Hasan A, Butt H, Ramzan A, Azam M, et al. Oxygen Generating Polymeric Nano Fibers That Stimulate Angiogenesis and Show Efficient Wound Healing in a Diabetic

Wound Model. International journal of nanomedicine. 2020;15:3511-3522.

19. Mirjalili M, Zohoori S. Review for application of electrospinning and electrospun nanofibers technology in textile industry. Journal of Nanostructure in Chemistry. 2016;6(3):207-213.

20. Memic A, Abudula T, Mohammed HS, Joshi Navare K, Colombani T, Bencherif SA. Latest Progress in Electrospun Nanofibers for Wound Healing Applications. ACS Applied Bio Materials. 2019;2(3):952-969.

21. Ahmadian-Fard-Fini S, Salavati-Niasari M, Ghanbari D. Hydrothermal green synthesis of magnetic Fe_3O_4-carbon dots by lemon and grape fruit extracts and as a photoluminescence sensor for detecting of E. coli bacteria. Spectrochimica Acta Part A: Molecular and Biomolecular Spectroscopy. 2018;203:481-493.

22. Rath G, Hussain T, Chauhan G, Garg T, Goyal AK. Collagen nanofiber containing silver nanoparticles for improved wound-healing applications. Journal of Drug Targeting. 2015;24(6):520-529.

23. Liao N, Unnithan AR, Joshi MK, Tiwari AP, Hong ST, Park C-H, et al. Electrospun bioactive poly (ε-caprolactone)–cellulose acetate–dextran antibacterial composite mats for wound dressing applications. Colloids Surf Physicochem Eng Aspects. 2015;469:194-201.

24. Barhoum A, Pal K, Rahier H, Uludag H, Kim IS, Bechelany M. Nanofibers as new-generation materials: From spinning and nano-spinning fabrication techniques to emerging applications. Applied Materials Today. 2019;17:1-35.

25. Haider A, Haider S, Kang I-K. A comprehensive review summarizing the effect of electrospinning parameters and potential applications of nanofibers in biomedical and biotechnology. Arabian Journal of Chemistry. 2018;11(8):1165-1188.

26. Liu S, Qin S, He M, Zhou D, Qin Q, Wang H. Current applications of poly(lactic acid) composites in tissue engineering and drug delivery. Composites Part B: Engineering. 2020;199:108238.

27. Shalumon KT, Anulekha KH, Girish CM, Prasanth R, Nair SV, Jayakumar R. Single step electrospinning of chitosan/poly(caprolactone) nanofibers using formic acid/acetone solvent mixture. Carbohydr Polym. 2010;80(2):413-419.

28. Jatoi AW, Ogasawara H, Kim IS, Ni Q-Q. Polyvinyl alcohol nanofiber based three phase wound dressings for sustained wound healing applications. Materials Letters. 2019;241:168-171.

29. Pal DB, Srivastava P, Mishra A, Giri DD, Srivastava KR, Singh P, et al. Synthesis and characterization of bio-composite nanofiber for controlled drug release. Journal of Environmental Chemical Engineering. 2017;5(6):5843-5849.

30. Barnthip N, Muakngam A. Preparation of Cellulose Acetate Nanofibers Containing Centella Asiatica Extract by Electrospinning Process as the Prototype of Wound-Healing Materials. Journal of Bionanoscience. 2014;8(4):313-318.

31. Xue J, Wu T, Dai Y, Xia Y. Electrospinning and Electrospun Nanofibers: Methods, Materials, and Applications. Chem Rev. 2019;119(8):5298-5415.

32. Xue J, Xie J, Liu W, Xia Y. Electrospun Nanofibers: New Concepts, Materials, and Applications. Acc Chem Res. 2017;50(8):1976-1987.

33. Wutticharoenmongkol P, Hannirojram P, Nuthong P. Gallic acid-loaded electrospun cellulose acetate nanofibers as potential wound dressing materials. Polym Adv Technol. 2019;30(4):1135-1147.

34. Unnithan AR, Gnanasekaran G, Sathishkumar Y, Lee YS, Kim CS. Electrospun antibacterial polyurethane–cellulose acetate–zein composite mats for wound dressing. Carbohydr Polym. 2014;102:884-892.

35. Vatankhah E, Prabhakaran MP, Jin G, Mobarakeh LG, Ramakrishna S. Development of nanofibrous cellulose acetate/gelatin skin substitutes for variety wound treatment applications. J Biomater Appl. 2013;28(6):909-921.

36. Brako F, Luo C, Craig DQM, Edirisinghe M. An Inexpensive, Portable Device for Point-of-Need Generation of Silver-Nanoparticle Doped Cellulose Acetate Nanofibers for Advanced Wound Dressing. Macromolecular Materials and Engineering. 2018;303(5):1700586.

37. Son WK, Youk JH, Park WH. Antimicrobial cellulose acetate nanofibers containing silver nanoparticles. Carbohydr Polym. 2006;65(4):430-434.

38. Jatoi AW, Kim IS, Ni Q-Q. Cellulose acetate nanofibers embedded with AgNPs anchored TiO_2 nanoparticles for long term excellent antibacterial applications. Carbohydr Polym. 2019;207:640-649.

39. Ghanbari D, Salavati-Niasari M, Khaghani S, Beshkar F. Preparation of Polyvinyl Acetate (PVAc) and PVAc–Ag–Fe_3O_4 Composite Nanofibers by Electro-spinning Method. Journal of Cluster Science. 2016;27(4):1317-1333.

40. Sung Hy, Wang Yy, Wan Cc. Preparation and Characterization of Poly(vinyl chloride-co-vinyl acetate)-Based Gel Electrolytes for Li-Ion Batteries. Journal of The Electrochemical Society. 1998;145(4):1207-1211.

41. Paladini F, Pollini M. Antimicrobial Silver Nanoparticles for Wound Healing Application: Progress and Future Trends. Materials (Basel, Switzerland). 2019;12(16):2540.

42. Diniz FR, Maia RCAP, Rannier L, Andrade LN, V Chaud M, da Silva CF, et al. Silver Nanoparticles-Composing Alginate/Gelatine Hydrogel Improves Wound Healing In Vivo. Nanomaterials (Basel, Switzerland). 2020;10(2):390.

43. Ibrahim HM, Reda MM, Klingner A. Preparation and characterization of green carboxymethylchitosan (CMCS) – Polyvinyl alcohol (PVA) electrospun nanofibers containing gold nanoparticles (AuNPs) and its potential use as biomaterials. Int J Biol Macromol. 2020;151:821-829.

44. Lau P, Bidin N, Islam S, Shukri WNBWM, Zakaria N, Musa N, et al. Influence of gold nanoparticles on wound healing treatment in rat model: Photobiomodulation therapy. Lasers in Surgery and Medicine. 2016;49(4):380-386.

45. Ahire JJ, Hattingh M, Neveling DP, Dicks LMT. Copper-Containing Anti-Biofilm Nanofiber Scaffolds as a Wound Dressing Material. PLoS One. 2016;11(3):e0152755-e0152755.

46. Alizadeh S, Seyedalipour B, Shafieyan S, Kheime A, Mohammadi P, Aghdami N. Copper nanoparticles promote rapid wound healing in acute full thickness defect via acceleration of skin cell migration, proliferation, and neovascularization. Biochemical and Biophysical Research Communications. 2019;517(4):684-690.

47. Ravanbakhsh H, Bao G, Mongeau L. Carbon nanotubes promote cell migration in hydrogels. Sci Rep. 2020;10(1):2543-2543.

48. Fatahian R, Mirjalili M, Khajavi R, Rahimi MK, Nasirizadeh N. Fabrication of antibacterial and hemostatic electrospun PVA nanofibers for wound healing. SN Applied Sciences. 2020;2(7).